Long-chain and very long-chain polyunsaturated fatty acids in ocular aging and age-related macular degeneration

Aihua Liu,* James Chang,[†] Yanhua Lin,* Zhengqing Shen,* and Paul S. Bernstein[1],*

Department of Ophthalmology and Visual Sciences,* Moran Eye Center, University of Utah School of Medicine, Salt Lake City, UT 84132; and Scientific Instruments Division,[†] ThermoFisher Scientific, San Jose, CA 95134

Abstract Retinal long-chain PUFAs (LC-PUFAs, C_{12}-C_{22}) play important roles in normal human retinal function and visual development, and some epidemiological studies of LC-PUFA intake suggest a protective role against the incidence of advanced age-related macular degeneration (AMD). On the other hand, retinal very long-chain PUFAs (VLC-PUFAs, $C_{n>22}$) have received much less attention since their identification decades ago, due to their minor abundance and more difficult assays, but recent discoveries that defects in VLC-PUFA synthetic enzymes are associated with rare forms of inherited macular degenerations have refocused attention on their potential roles in retinal health and disease. We thus developed improved GC-MS methods to detect LC-PUFAs and VLC-PUFAs, and we then applied them to the study of their changes in ocular aging and AMD. With ocular aging, some VLC-PUFAs in retina and retinal pigment epithelium (RPE)/choroid peaked in middle age. Compared with age-matched normal donors, docosahexaenoic acid, adrenic acid, and some VLC-PUFAs in AMD retina and RPE/choroid were significantly decreased, whereas the ratio of n-6/n-3 PUFAs was significantly increased.■ All these findings suggest that deficiency of LC-PUFAs and VLC-PUFAs, and/or an imbalance of n-6/n-3 PUFAs, may be involved in AMD pathology.—Liu, A., J. Chang, Y. Lin, Z. Shen, and P. S. Bernstein. **Long-chain and very long-chain polyunsaturated fatty acids in ocular aging and age-related macular degeneration.** *J. Lipid Res.* 2010. 51: 3217–3229.

Supplementary key words retina • retinal pigment epithelium (RPE)/choroid • eye

The biochemical profile of FAs in human retina was first reported over 45 years ago when Futterman and Andrews (1) identified five major FAs in human retina, including docosahexaenoic acid (DHA, 22:6n-3), arachidonic acid (AA, 20:4n-6), stearic acid (SA, 18:0), oleic acid (OA, 18:1), and palmitic acid (PA, 16:0), all of which belong to the long-chain FA (LC-FA, C_{12}-C_{22}) family. Subsequent studies demonstrated that DHA and AA are the major components of human and vertebrate retinal long-chain PUFAs (LC-PUFAs), and the highest content of LC-PUFAs is found in human and vertebrate retinal rod outer segment membranes (2–4). Their high content and specific tissue distribution suggest that LC-PUFAs have an important functional role in the retina.

Human clinical studies and animal studies involving dietary manipulation in rats (5, 6) have shown that LC-PUFAs are important for the development and function of the central nervous system, particularly the visual system (7). DHA prevented photoreceptor apoptosis caused by oxidative damage (8) and promoted differentiation of developing photoreceptors in culture (9). DHA also has significant effects on photoreceptor membranes and neurotransmitters involved in the signal transduction process, rhodopsin activation, rod and cone development, neuronal dendritic connectivity, and functional maturation of the central nervous system (10). Low plasma and blood cell lipid DHA have been linked to increased risk of poor visual and neural development in infants and children (11, 12). Depletion of DHA, AA, or eicosapentaenoic acid (EPA) from the retina interferes with normal neurogenesis, neurological function, and visual signaling pathways, impairs vision and visual learning tasks, and leads to an abnormal elec-

Abbreviations: AA, arachidonic acid; AMD, age-related macular degeneration; CEP, carboxyethyl pyrrole; DHA, docosahexaenoic acid; EFA, essential FA; EI, electron ionization; EPA, eicosapentaenoic acid; FAME, fatty acid methyl ester; LA, linoleic acid; LC-FA, long-chain FA; LCI, liquid chemical ionization; LC-PUFA, long-chain PUFA; NIST, National Institute of Standards and Technology; OA, oleic acid; PA, palmitic acid; RPE, retinal pigment epithelium; SA, stearic acid; SIM, selected ion monitoring; VLC-PUFA, very long-chain PUFA.
[1] To whom correspondence should be addressed.
   e-mail: paul.bernstein@hsc.utah.edu

troretinogram (13–20). Thus, it is clear that LC-PUFAs play an essential role in the development of vision during human early life (16, 21). In later human life, some epidemiological studies of LCn-3PUFA intake on the prevalence of advanced age-related macular degeneration (AMD) suggest a protective relationship (21–27), and Hubbard et al. (28) showed a protective effect of DHA and EPA intake in autosomal dominant Stargardt disease. Their role in the prevention of inherited retinal degenerations such as retinitis pigmentosa is more ambiguous (29).

Although retinal LC-PUFAs have received extensive attention over the past decades, very long-chain PUFAs (VLC-PUFAs, $C_{n>22}$) (30, 31) are also found in mammalian tissues, but they occur in only a restricted number of organs such as retina, testes, thymus, and brain in a low amount and their saturated analogs are essential parts of the skin moisture barrier (32, 33). Unlike DHA, AA, EPA, and their precursors, VLC-PUFAs are not present in a normal human diet (34), but they can be synthesized from precursors such as 22:4n-6 and 22:5n-3 via a biochemical pathway (supplementary Fig. I) featuring the enzymes of the elongation of very long-chain FAs family along with β-oxidases and desaturases (31, 35–37). Defects in the elongation of the very long-chain FAs-4 (*ELOVL4*) gene are associated with autosomal dominant Stargardt macular dystrophy in the heterozygous state and neonatal demise in transgenic mice due to loss of skin barrier function in the homozygous state. VLC-PUFAs are of particular interest, because they exhibit a unique hybrid structure combining a proximal end with typical saturated FA character and a distal end more characteristic of common PUFAs (35, 36). They may play important roles in biological systems that cannot be performed by the more common saturated and unsaturated LC-FAs (35, 36); however, their greater length and minor abundance make them unusually difficult to analyze (36), which means that VLC-PUFAs have often been overlooked since their discovery (33, 38).

In this study, we optimized analytical methods to detect LC-PUFAs and VLC-PUFAs in human retina and retinal pigment epithelium (RPE)/choroid. We applied these methods to explore possible retinal functions of LC-PUFAs and VLC-PUFAs, and we assessed how their levels change in ocular aging and AMD.

MATERIALS AND METHODS

Materials and dissections

Human donor eyes were obtained from the Utah Lions Eye Bank within 26 h after death, and donor demographic data are shown in **Table 1**. All experimental procedures including tissue procurement and distribution were conducted according to the tenets of the Declaration of Helsinki. The time between donor death and enucleation was <4 h. Dissections of donor eyeballs were carried out 6–26 h [(mean ± SD) 17.4 ± 2.3 h] (Table 1) after donor death in a dim-light environment. The posterior pole of donor eyeballs was placed on a back-lit table and observed under a dissecting microscope to prepare the tissue needed in the present study. Normal donor eyes were inspected under magnifi-

cation to assure that no significant macular pathology was present. Likewise, eyes from donors with a clinical history of AMD were inspected to confirm that their macular characteristics correlated with clinical examinations recorded prior to death. After removal of the vitreous body, the whole retina and the RPE/choroid layer were carefully separated with forceps. Wet sample weights were recorded for all collected tissues after blotting excess moisture. All samples were immediately blanketed with argon and stored at −80°C until further analysis.

All analytical solutions such as methanol, hydrochloric acid, isopropanol, and n-hexane were GC-MS grade reagents and were purchased from Fisher Scientific (Pittsburgh, PA). All standards such as tridecanoic acid (C_{13}) and hentriacontanoic acid (C_{31}) were purchased from Sigma-Aldrich (St. Louis, MO). Silica gel glass-encased solid phase extraction cartridges (500 mg/6 ml) were purchased from Sorbent Technology (Atlanta, GA).

Sample preparation including total lipid extraction, fatty acid methyl ester formation, and sample cleaning with solid-phase extraction

Samples were removed from the −80°C freezer and placed on ice. Tridecanoic acid (20 μg) and hentriacontanoic acid (1 μg) were added as the internal standards. Total lipid was extracted from whole retina or RPE/choroid tissue based on a previously described method (39). The samples were probe sonicated with 0.5 ml hexane:isopropanol (3:2) in a glass bottle. Then hexane:isopropanol (3:2) was added to a final volume equivalent to 40 times the sample weight (i.e., 1 g in 40 ml of solvent mixture). The sample bottles sealed under argon with Teflon-lined caps were bath sonicated for 20 min at room temperature. The extract was then centrifuged at 5,000 rpm for 5 min, and the upper layer was dried under vacuum.

The dried film dissolved in 200 μl hexane and 2 ml 8% HCl/MeOH was sealed under argon with Teflon-lined caps and heated at 80°C for 4 h to form fatty acid methyl esters (FAMEs) (36), then cooled on ice. The cool reacted solution was extracted three times with 1 ml distilled water and 2 ml hexane. The hexane layers were combined and dried under vacuum.

Silica gel glass-encased solid-phase extraction cartridges were subsequently used to clean the FAME extracts. The cartridge was activated by 6 ml of hexane before loading samples. The crude FAME extract was dissolved in 200 μl of hexane and loaded onto the activated cartridge. Then 6 ml hexane was used to wash the cartridge, and the eluate was discarded. Then the FAMEs were eluted by 5 ml hexane:ether (8:2), and the eluate was evaporated to dryness under vacuum. The dry film was dissolved in 200 μl of hexane and centrifuged for 3 min at 14,000 rpm to remove particles prior to GC-MS analysis. Then 1 μl of sample was injected into the GC-MS instrument for LC-PUFA analysis. The sample was dried under vacuum again and redissolved in 30 μl of hexane. Then 5 μl samples were injected into the GC-MS instrument for VLC-PUFA analysis.

GC-MS instrumentation and chromatographic conditions

The Thermo Trace GC-DSQ system (ThermoFisher Scientific, Waltham, MA) consisted of an automatic sample injector (AI 3000), gas chromatograph, single quadrupole mass detector, and an analytical workstation. The chromatographic separation was carried out with an Rxi-5MS-coated 5% diphenyl/95% dimethyl polysiloxane capillary column (30 m × 0.25 mm inner diameter, 0.25 μm film thickness, Restek, Bellefonte, PA).

For LC-FA analyses, we used the following MS conditions (Method A): 1 μl from a 200 μl sample was injected into the GC-MS using a splitless mode; the septum purge was on; and the injector temperature was set at 200°C. The column temperature was programmed as follows: initial temperature 60°C; 5 degrees/

TABLE 1. The demographic information of all samples

Sample no.	Group	Average Age[a]	Gender (M/F)	Age (y)	Delay of Collection after Death (h)	Weight of Retina (g)	Weight of RPE/Choroid (g)	Eye Disease History	Cause of Death
1	Young age group	16.4 ± 3.6	M	17	14	0.1547	0.0953	No	Heart failure
2			F	22	21	0.0879	0.1208	No	Respiratory collapse
3			F	12	16	0.1149	0.1223	No	Multiple sclerosis
4			F	15	22	0.0873	0.1006	No	Anoxic brain injury
5			M	16	22	0.1149	0.1223	No	Blunt force head trauma
6	Middle age group	38.2 ± 6.2	M	36	26	0.0917	0.0867	No	Respiratory failure
7			M	38	26	0.0846	0.0775	No	Aspiration pneumonia
8			M	49	13	0.1157	0.1181	No	Respiratory arrest
9			M	39	16	0.1099	0.1090	No	Myocardial infarction
10			M	37	6	0.0799	0.0990	No	End-stage renal failure
11			M	30	8	0.1056	0.0976	No	Congestive heart failure
12	Old age group	74.0 ± 3.4	M	77	15	0.1164	0.1363	No	Trauma
13			F	78	23	0.1332	0.0992	No	Cerebrovascular accident
14			M	72	20	0.1550	0.1089	No	Cerebrovascular accident
15			F	70	7	0.1242	0.1378	No	Cerebrovascular accident
16			F	73	17	0.1542	0.1678	No	Amyotrophic lateral sclerosis
17	Age-matched AMD group	77.2 ± 6.4	M	78	23	0.1538	0.1375	AMD	Cancer
18			F	70	23	0.1123	0.1462	AMD	Myocardial infarction
19			M	75	22	0.1557	0.1562	AMD	Lymphoma
20			M	73	17	0.0947	0.1008	AMD	Respiratory failure
21			M	81	8	0.1357	0.1313	AMD[b]	Circulatory collapse
22			F	84	22	0.2557	0.2562	AMD	Renal failure
23			F	87	18	0.1671	0.1395	AMD[b]	Respiratory failure, breast cancer
24			M	70	8	0.1222	0.0722	AMD	Circulatory collapse

[a] Average ± SD.
[b] These AMD patients had exudative AMD. All other AMD patients had early to intermediate dry AMD with drusen and pigmentary changes but no history of geographic atrophy or exudative disease.

JOURNAL OF LIPID RESEARCH

ASBMB

min to 170°C; 1 degree/min to 180°C; 2 degrees/min to 240°C; 4 degrees/min to 290°C; and a hold at 290°C for 5 min. Transfer line temperature was 290°C. Helium was used as the carrier gas at a flow rate of 1.0 ml/min. MS conditions were as follows: electron ionization (EI) mode; ion source temperature, 200°C; multiplier voltage, 1,182 V; solvent delay, 5 min. All data were obtained by collecting the full-scan mass spectra within the scan range of 50–650 amu. Compounds were identified by comparing their mass spectra with those in the National Institute of Standards and Technology (NIST) library. Authentic reference compounds were used to calculate the weight percentage of every peak.

For VLC-PUFAs, we used the following MS conditions (Method B): 5 µl from 30 µl of sample was injected onto the GC-MS using a splitless mode; the septum purge was on; and the injector temperature was set at 200°C. The column temperature was programmed as follows: initial temperature, 60°C; 10 degrees/min to 240°C; 1 degree/min to 290°C; and 290°C for 5 min. Transfer line temperature was 290°C. Helium was used as the carrier gas at a flow rate of 1.5 ml/min. Both liquid chemical ionization (LCI) and EI modes were used to identify VLC-PUFAs, whereas only the EI mode was used for quantification. The MS conditions for LCI were as follows: ion source temperature, 180°C; multiplier voltage, 1,182 V; solvent delay, 22 min; selected ion monitoring (SIM) mode with molecular weights plus one ion; acetonitrile flow rate, 0.1 µl/min. The MS conditions under EI were as follows: ion source temperature, 200°C; multiplier voltage, 1,182 V; solvent delay, 22 min, SIM mode with m/z 79, 108, and 150. Comparison was made by normalizing the each peak area with the internal standard and the retina or RPE/choroid sample weight. The formula to calculate the values in Tables 4 and 5 and Fig. 5 is as follows:

$$Value = \frac{PA}{RF \times W \times 10^5} \qquad (Formula\ 1)$$

$$RF = \frac{PA_a}{PA_b} \qquad (Formula\ 2)$$

In the first formula, PA, RF, and W are the peak area of target peak, response factor, and sample weight with grams as the unit. In the second formula, PA_a is the peak area of IS in the sample, and PA_b is the peak area of fresh IS solution at the same concentration.

Statistical analysis

Quantitative data were expressed as mean ± SEM, and they were analyzed for statistical significance using one-way ANOVA in an SPSS statistical package (SPSS Inc., Chicago, IL, version 12.0). The number of samples used in each group is presented in the figure legends. $P < 0.05$ was defined as the level of significance.
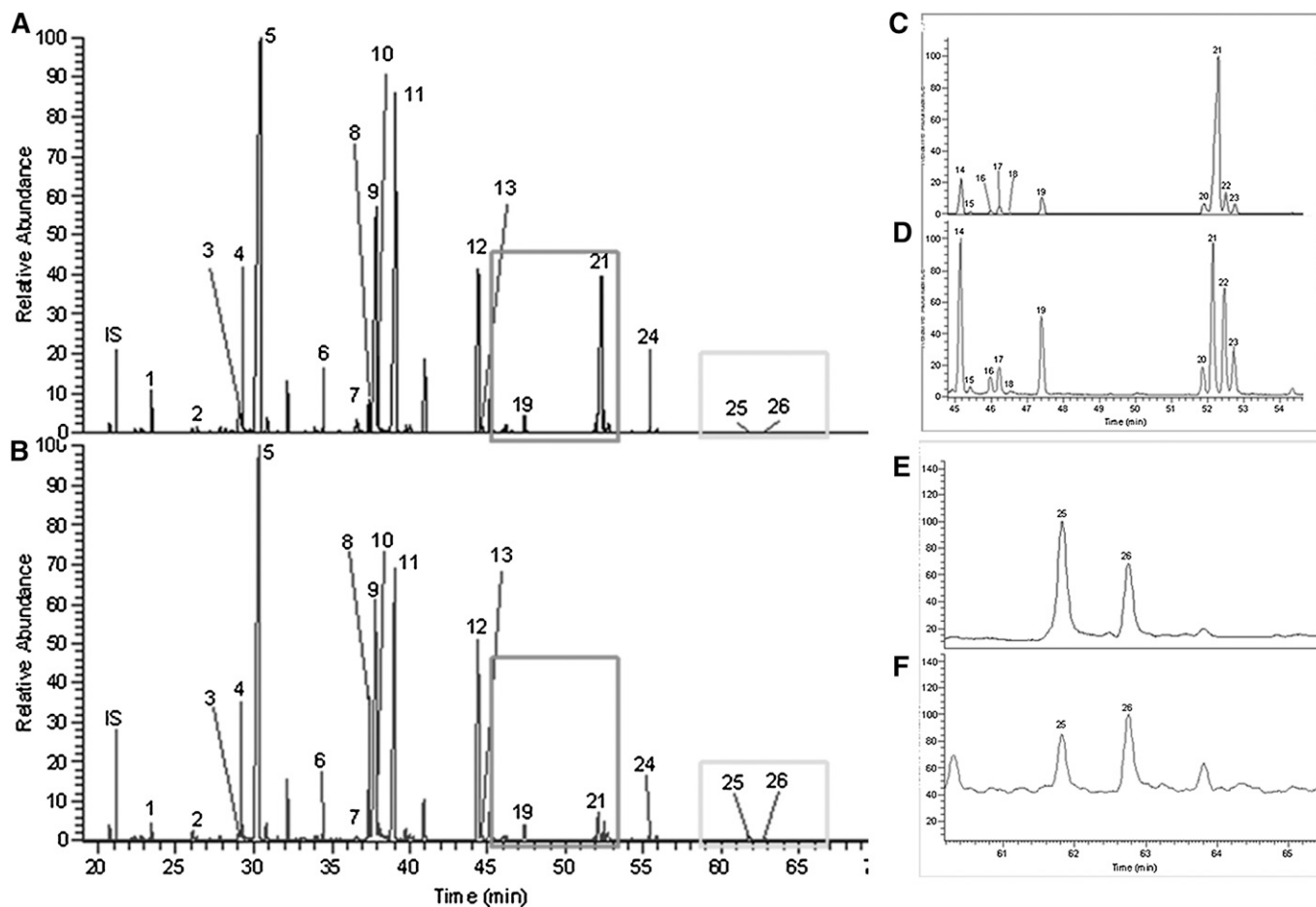

Fig. 1. GC-MS total ion chromatograms (TIC) of LC-FAs in retina and RPE/choroid using Method A. MS was performed in full scan mode (50–650 amu). A and B are examples of LC-FA chromatograms of human whole retina and RPE/choroid, respectively; C and D are amplified chromatograms corresponding to the larger rectangles in A and B, respectively; E and F are amplified chromatograms corresponding to the smaller rectangles in A and B, respectively. IS: internal standard (tridecanoic acid; C_{13}). Peak nos. 1–26 were identified according to authentic standards and the NIST library. Further structure information is shown in Tables 2 and 3.

RESULTS

The characteristics of the various donor eyes such as the time point of tissue collection, the ocular condition (AMD or normal), sex, age, and tissue weight are described in Table 1. Retina and RPE/choroid samples were grouped into three age categories: young (age range 12–22 years, 16.4 ± 3.6), middle (age range 30–49 years, 38.2 ± 6.2), and old (age range 70–78 years, 74.0 ± 3.4) and age-matched AMD (age range 70–87 years, mean age ± SD, 77.2 ± 6.4).

Method development

Because these lipids, especially VLC-PUFAs, are difficult to analyze, we had to optimize the assay conditions. Although TLC is a commonly employed method for purification of FAMEs formed after transesterification (33, 36, 40), it is cumbersome, solvent consuming, and time intensive. To circumvent these disadvantages, TLC was replaced by solid-phase extraction in our study to purify the samples following total lipid extraction and methyl esterification. Cholesterol is the main endogenous substance that can interfere with the analysis of FAME. Therefore, we chose silica gel glass-encased cartridges to remove it (supplementary Fig. II). Silica gel cartridges function in the same way as TLC but with higher recovery and speed, which helps to minimize lipid peroxidation that could occur during TLC analysis.

LC-FAs were identified and quantified by MS using the full-scan EI mode (Method A), because all information about LC-FAs in the NIST library was acquired in this manner. Unfortunately, EI is less valuable for identification of VLC-PUFAs, because they all exhibit the same base peak of m/z 79 (36), no standards are commercially available, and they are not a part of the NIST library. Therefore, we used the LCI mode to identify VLC-PUFAs. Unlike the EI mode, the base peak of each VLC-PUFA obtained under the LCI mode corresponded to the molecular weight of the lipid (supplementary Fig. III). Furthermore, n-3 and VLCn-6PUFAs can be distinguished under EI mode based on the ratio of 108 and 150 m/z (41) (supplementary Fig. IV). We set the mass detector to be off at the first 22 min due to the very high concentration of the LC-FAs that come out before 22 min and saturate the detector. Quantification of the VLC-PUFAs was performed using SIM of the EI mode (Method B).

In principle, the internal standard should have not only similar chemical structure and characteristics with the target compounds, but also it should be absent in the samples. So far, there is no ideal unsaturated internal standard for VLC-PUFA analysis on the market. Therefore, we chose hentriacontanoic acid, a saturated VLC-FA, as the best available internal standard for the measurement of VLC-PUFAs in method B.

TABLE 2. LC-FA composition from the whole retinas collected from young, middle, and old age and age-matched AMD human donors

Peak no.[a]	RT (min)[b]	FAs[c]	Common Name	Mole % of Total FAs[d]			
				Young Age Group	Middle Age Group	Old Age Group	Age-Matched AMD Group
1	23.51	14:0	Tetradecanoic acid	0.50 ± 0.06	0.60 ± 0.06	0.61 ± 0.05	0.81 ± 0.09
2	26.42	15:0	Pentadecanoic acid	0.15 ± 0.05	0.12 ± 0.02	0.11 ± 0.01	0.21 ± 0.04
3	29.06	16:1n-9	7-Hexadecenoic acid	0.91 ± 0.14	0.66 ± 0.09	0.62 ± 0.04	0.76 ± 0.09
4	29.24	16:1n-7	9-Hexadecenoic acid	0.48 ± 0.03	0.49 ± 0.05	0.36 ± 0.03	0.50 ± 0.07
5	30.39	16:0	PA	15.98 ± 1.18	16.37 ± 1.37	16.62 ± 0.79	19.64 ± 1.79
6	34.45	17:0	Heptadecanoic acid	0.12 ± 0.04	0.08 ± 0.02	0.07 ± 0.02	0.14 ± 0.02
7	36.61	18:3n-3	α-Linolenic acid	0.39 ± 0.07	0.24 ± 0.06	0.24 ± 0.05	0.30 ± 0.04
8	37.38	18:2-6	LA	1.63 ± 0.13	2.12 ± 0.15	1.93 ± 0.20	2.35 ± 0.24
9	37.85	18:1n-9	OA	14.88 ± 0.46	16.04 ± 1.56	14.53 ± 1.11	17.14 ± 1.38
10	38.02	18:1n-7	11-Octadecenoic acid	2.79 ± 0.17	2.83 ± 0.12	2.57 ± 0.25	3.08 ± 0.23
11	39.18	18:0	Octadecanoic acid/SA	14.80 ± 1.15	13.50 ± 0.46	13.91 ± 0.53	15.45 ± 0.98
12	44.47	20:4n-6	AA	13.43 ± 0.34	14.26 ± 0.64	14.04 ± 0.47	13.04 ± 0.36
13	44.64	20:5n-3	5,8,11,14,17-EPA	0.27 ± 0.03	0.28 ± 0.03	0.24 ± 0.04	0.35 ± 0.05
14	45.18	20:3n-6	8,11,14- Eicosatrienoic acid	2.38 ± 0.28	2.63 ± 0.14	2.29 ± 0.27	2.57 ± 0.26
15	45.44	20:2n-7	8,11-Eicosadienoic acid	0.09 ± 0.03	0.13 ± 0.05	0.10 ± 0.03	0.18 ± 0.02
16	45.99	20:2n-9	11,14-Eicosadienoic acid	0.09 ± 0.02	0.09 ± 0.02	0.14 ± 0.02	0.16 ± 0.04
17	46.23	20:1n-9	9-Eicosenoic acid	0.24 ± 0.04	0.29 ± 0.04	0.37 ± 0.04	0.55 ± 0.14
18	46.51	20:1n-7	11-Eicosenoic acid	0.17 ± 0.06	0.10 ± 0.05	0.03 ± 0.00	0.04 ± 0.01
19	47.42	20:0	Eicosanoic acid	0.65 ± 0.03	0.66 ± 0.01	0.82 ± 0.09	1.11 ± 0.15
20	51.90	22:5n-6	4,7,10,13,16-Docosapentaenoic acid	1.42 ± 0.33	1.03 ± 0.28	1.41 ± 0.31	1.02 ± 0.17
21	52.30	22:6n-3	4,7,10,13,16,19-DHA	23.74 ± 1.48	21.75 ± 2.78	23.01 ± 1.65	16.49 ± 0.62[e]*
22	52.50	22:4n-6	7,10,13,16-Docosatetraenoic acid (adrenic acid)	2.21 ± 0.40	2.53 ± 0.38	2.82 ± 0.37	1.61 ± 0.29[e]*
23	52.76	22:5n-3	7,10,13,16,19-Docosapentaenoic acid	1.52 ± 0.29	1.94 ± 0.36	1.77 ± 0.34	1.24 ± 0.25
24	55.39	22:0	Behenic acid	0.31 ± 0.02	0.40 0.03	0.41 ± 0.04	0.41 ± 0.03
25	61.83	24:1n-9	15-Tetracosenoic acid	0.66 ± 0.15	0.56 ± 0.10	0.71 ± 0.13	0.60 ± 0.15
26	62.75	24:0	Tetracosanoic acid	0.20 ± 0.03	0.31 ± 0.03	0.28 ± 0.04	0.25 ± 0.04
Ratio of AA/DHA				0.58 ± 0.05	0.76 ± 0.17	0.63 ± 0.06	0.79 ± 0.02[e]*
Ratio of n-6/n-3 LC-PUFAs				0.83 ± 0.05	1.05 ± 0.20	0.91 ± 0.06	1.13 ± 0.04[e]*

[a] Peak no. was shown in chromatograms of Fig. 1.

[b] Retention time.

[c] Number of carbon atoms: number of double bonds, the position of first double bound.

[d] Mean ± SEM; young age group: n = 5, middle age group: n = 6, old age group: n = 5, age-matched AMD group: n = 8.

[e]* Significant differences ($P < 0.05$) between old age and age-matched AMD group.

Separation of LC-FAs from retina and RPE/choroid

Full scan (50–650 amu) MS under EI mode was used to detect LC-FAs. The chromatogram is shown in **Fig. 1**. Twenty-six LC-FAs ranging from 14:0 to 24:0 were identified in retina and RPE/choroid after comparison with the NIST library and standards. Their retention times, structures, and common names are listed in **Tables 2** and **3**. The retention time variation of individual peaks for different runs within 1 day was ± 0.1 min.

LC-FAs in retina

In whole retina, five major FAs (PA, OA, SA, AA, and DHA; peaks 5, 9, 11, 12, and 21, respectively, in Fig. 1) predominated, accounting for 82.09% in total. EPA, one of the major components of fish oil, accounted for <0.29% of retinal lipids. There were no significant differences between young, middle, and old age groups for the 26 LC-FAs listed. When comparing AMD donors to an age-matched old age group, the concentrations of two LC-PUFAs, DHA and adrenic acid, were significantly decreased in the presence of AMD ($P < 0.05$). The ratios of AA/DHA and n-6/n-3 in age-matched AMD retinas (0.79 ± 0.02 and 1.13 ± 0.04) significantly increased compared with the old age group (0.63 ± 0.06 and 0.91 ± 0.06).

LC-FAs in RPE/choroid

In RPE/choroid, linoleic acid (LA) replaced DHA as one of the five major FAs. Together, PA, LA, OA, SA, and AA (peaks 5, 8, 9, 11, and 12, respectively, in Fig. 1) accounted for 78.78% of total lipids. The content of DHA was low, more variable, and accounted for only 2.20–14.96% of RPE/choroid lipids. After comparing the major FAs in retina and RPE/choroid, we found that the percentage of DHA was much lower and more variable in RPE/choroid (average $4.92 \pm 0.65\%$) than in retina (average $20.67 \pm 1.02\%$) ($P < 0.05$), whereas LA was much higher in RPE/choroid (average $12.98 \pm 0.72\%$) than in retina (average $2.06 \pm 0.11\%$) ($P < 0.05$).

In RPE/choroid, the concentration of LA (peak 8) was significantly higher in the old age group relative to the middle age group ($P < 0.05$). Our results further showed that DHA and adrenic acid were significantly different between the old age group and the age-matched AMD group. In particular, DHA and adrenic acid were higher in the old age group relative to the age-matched AMD group ($P < 0.05$), whereas DHA peaked in the middle age group ($P < 0.05$). The ratios of AA/DHA and n-6/n-3 in age-matched AMD retinas (6.41 ± 0.41 and 7.97 ± 0.51) were significantly higher than the old age control group (3.90 ± 0.19 and 5.22

TABLE 3. LC-FA composition from RPE/choroid collected from young, middle, and old age and age-matched AMD human donors

Peak no.[a]	RT (min)[b]	FAs[c]	Common Name	Mole % of Total FAs[d]			
				Young Age Group	Middle Age Group	Old Age Group	Age-Matched AMD Group
1	23.51	14:0	Tetradecanoic acid	0.51 ± 0.07	0.60 ± 0.07	0.52 ± 0.06	0.75 ± 0.10
2	26.42	15:0	Pentadecanoic acid	0.15 ± 0.00	0.12 ± 0.01	0.13 ± 0.01	0.18 ± 0.03
3	29.06	16:1n-9	7-Hexadecenoic acid	0.41 ± 0.03	0.48 ± 0.05	0.48 ± 0.04	0.68 ± 0.14
4	29.24	16:1n-7	9-Hexadecenoic acid	0.70 ± 0.08	1.03 ± 0.19	0.96 ± 0.10	1.20 ± 0.14
5	30.39	16:0	PA	18.41 ± 1.00	17.77 ± 1.43	16.49 ± 0.94	19.20 ± 0.81
6	34.45	17:0	Heptadecanoic acid	0.17 ± 0.05	0.15 ± 0.03	0.11 ± 0.03	0.21 ± 0.03
7	36.61	18:3n-3	α-Linolenic acid	0.20 ± 0.05	0.22 ± 0.05	0.30 ± 0.04	0.34 ± 0.06
8	37.38	18:2n-6	LA	10.33 ± 0.69	9.46 ± 0.02	13.80 ± 0.61[f]*	16.31 ± 2.25
9	37.85	18:1n-9	OA	18.15 ± 0.44	18.94 ± 1.31	19.11 ± 1.31	20.81 ± 1.51
10	38.02	18:1n-7	11-Octadecenoic acid	1.92 ± 0.13	2.39 ± 0.30	2.07 ± 0.16	2.45 ± 0.17
11	39.18	18:0	Octadecanoic acid/SA	10.92 ± 0.51	9.80 ± 0.38	9.24 ± 0.26	9.20 ± 0.27
12	44.47	20:4n-6	AA	20.89 ± 2.87	17.61 ± 1.75	19.14 ± 0.30	17.19 ± 1.10
13	44.64	20:5n-3	5,8,11,14,17-EPA	0.28 ± 0.03	0.34 ± 0.05	0.38 ± 0.04	0.49 ± 0.09
14	45.18	20:3n-6	8,11,14- Eicosatrienoic acid	2.70 ± 0.26	2.64 ± 0.25	3.08 ± 0.51	2.33 ± 0.19
15	45.44	20:2n-7	8,11-Eicosadienoic acid	0.14 ± 0.06	0.16 ± 0.06	0.11 ± 0.02	0.21 ± 0.04
16	45.99	20:2n-9	11,14- Eicosadienoic acid	0.13 ± 0.05	0.13 ± 0.04	0.19 ± 0.05	0.11 ± 0.02
17	46.23	20:1n-9	9-Eicosenoic acid	0.13 ± 0.04	0.20 ± 0.02	0.16 ± 0.03	0.20 ± 0.01
18	46.51	20:1n-7	11-Eicosenoic acid	0.03 ± 0.01	0.03 ± 0.00	0.03 ± 0.01	0.02 ± 0.00
19	47.42	20:0	Eicosanoic acid	0.71 ± 0.02	0.57 ± 0.05	0.62 ± 0.07	0.62 ± 0.04
20	51.90	22:5n-6	4,7,10,13,16-Docosapentaenoic acid	0.96 ± 0.15	0.97 ± 0.27	0.93 ± 0.19	0.49 ± 0.07
21	52.30	22:6n-3	4,7,10,13,16,19-DHA	4.13 ± 0.44	9.22 ± 1.95[e]*	4.94 ± 0.18[f]*	2.72 ± 0.15[g]*
22	52.50	22:4n-6	7,10,13,16-Docosatetraenoic acid (adrenic acid)	3.67 ± 0.45	3.10 ± 0.53	3.22 ± 0.34	1.43 ± 0.11[g]*
23	52.76	22:5n-3	7,10,13,16,19-Docosapentaenoic acid	2.12 ± 0.48	2.27 ± 0.47	2.09 ± 0.26	1.31 ± 0.14
24	55.39	22:0	Behenic acid	0.76 ± 0.06	0.61 ± 0.06	0.64 ± 0.06	0.61 ± 0.04
25	61.83	24:1n-9	15-Tetracosenoic acid	0.48 ± 0.15	0.51 ± 0.19	0.49 ± 0.10	0.42 ± 0.03
26	62.75	24:0	Tetracosanoic acid	0.97 ± 0.14	0.70 ± 0.09	0.74 ± 0.06	0.54 ± 0.08
Ratio of AA/DHA				5.24 ± 0.49	2.42 ± 0.64[e]*	3.90 ± 0.19[f]*	6.41 ± 0.41[g]*
Ratio of n-6/n-3 LC-PUFAs				5.84 ± 0.42	3.23 ± 0.65[e]*	5.22 ± 0.22[f]*	7.97 ± 0.51[g]*

[a] Peak no. was shown in chromatograms of Fig. 1.
[b] Retention time.
[c] Number of carbon atoms: number of double bonds, the position of first double bound.
[d] Mean ± SEM; young age group: n = 5, middle age group: n = 6, old age group: n = 5, age-matched AMD group: n = 8.
[e]* Significant differences ($P < 0.05$) between young and middle age group.
[f]* Significant differences ($P < 0.05$) between middle and old age group.
[g]* Significant differences ($P < 0.05$) between old and age-matched AMD age group.

± 0.22), whereas the ratios of AA/DHA and n-6/n-3 in middle age RPE/choroid were significantly lower compared with young and old age retinas.

Separation of VLC-PUFAs from retina and RPE/choroid

Typical GC-MS chromatograms of human retina lipids using EI and LCI detection are shown in **Figs. 2** and **3**, respectively. The same column and same temperature programs were used for both EI and LCI, so the retention times of the VLC-PUFAs were the same under both detection conditions. Twenty-one VLC-PUFAs were identified in human retina and RPE/choroid, and these 21 VLC-PUFAs belong to six groups: C_{24}, C_{26}, C_{28}, C_{30}, C_{32}, and C_{34}. Each group had several subtypes. The C_{24} group had 24:5n-6, 24:6n-3, 24:n-6, and 24:5n-3; the C_{26} group had 26:5n-6, 26:6n-3, 26:4n-6, and 26:5n-3; the C_{28} group had 28:6n-3, 28:4n-6, and 28:5n-3; the C_{30} group

had 30:6n-3, 30:4n-6, and 30:5n-3; the C_{32} group had 32:5n-6, 32:6n-3, 32:4n-6, and 32:5n-3; and the C_{34} group had 34:6n-3, 34:4n-6, and 34:5n-3.

VLC-PUFAs in retina

The results of retinal VLC-PUFA analyses are shown in **Table 4** and **Fig. 4**A. In the whole retina, the concentrations of 28:4n-6, 30:6n-3, 30:5n-3, 32:4n-6, and 32:5n-3 peaked in the middle age group ($P < 0.05$). The concentrations of some VLC-PUFAs including 24:6n-3, 26:4n-6, 28:4n-6, 28:5n-3, 30:4n-6, 32:5n-6, 32:6n-3, 32:5n-3, and 34:4n-6 were significantly higher in the normal old age group compared to the age-matched AMD group ($P < 0.05$). Other VLC-PUFAs also showed increased average levels in the normal old group compared with the age-matched AMD group, but these differences were not
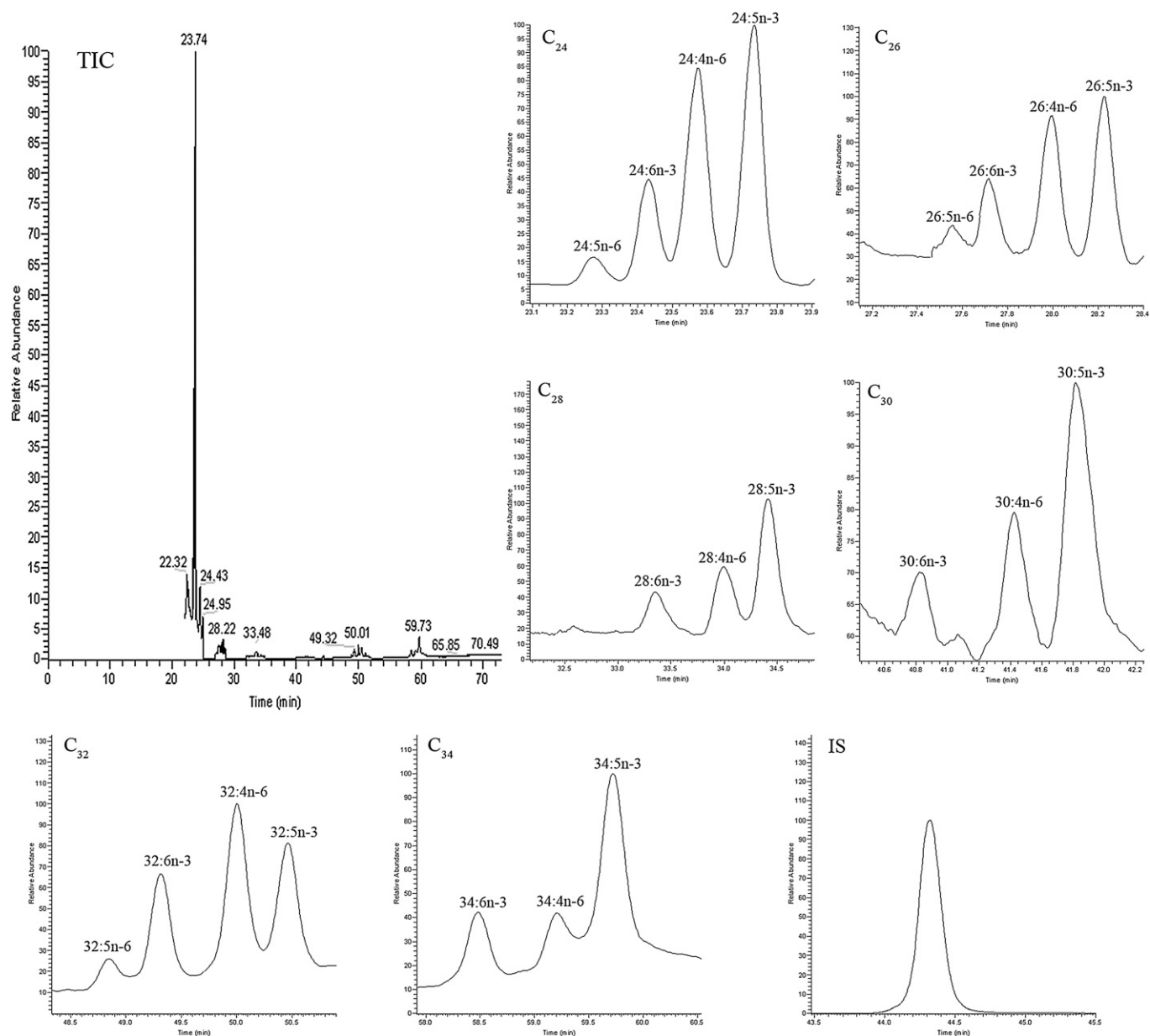
Fig. 2. Typical SIM GC-MS chromatograms of C_{24}-C_{34} VLC-PUFAs analyzed from human retina using Method B in the EI mode. IS: internal standard (hentriacontanoic acid; C_{31}); TIC: total ion chromatogram.
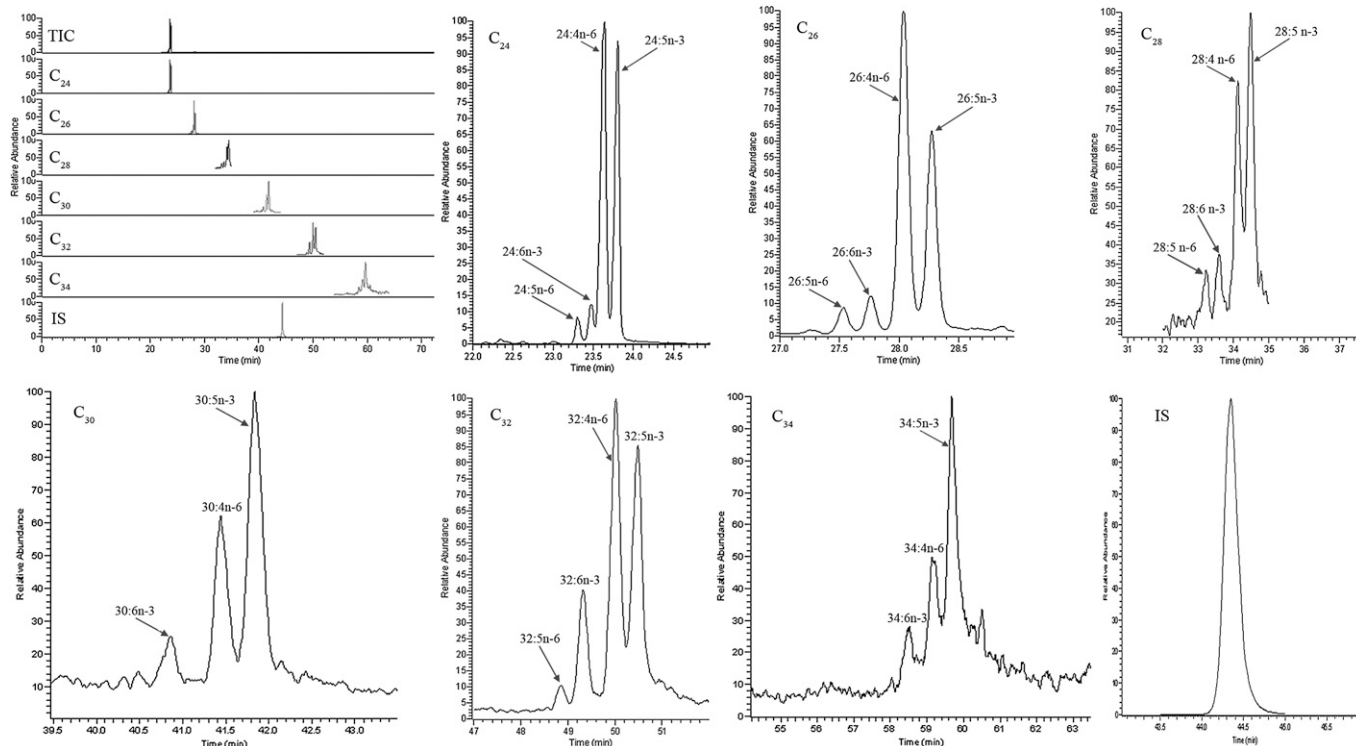
Fig. 3. Typical SIM GC-MS chromatograms of C_{24}-C_{34} VLC-PUFAs analyzed from human retina using Method B in the LCI mode. IS: internal standard (hentriacontanoic acid; C_{31}); TIC: total ion chromatogram.

significant. The ratios of n-6/n-3 VLC-PUFAs and the sum of all VLC-PUFAs in old age group retinas (0.83 ± 0.09 and 3203 ± 535) were significantly decreased compared with the ratio and sum in age-matched AMD retinas (1.24 ± 0.10 and 1355 ± 268) ($P < 0.05$).

VLC-PUFAs in RPE/choroid

The results of the RPE/choroid VLC-PUFA analysis are shown in **Table 5** and Fig. 4B. C_{24}-C_{26} VLC-PUFAs were detectable in individual RPE/choroid samples, whereas C_{30}-C_{34} VLC-PUFAs were detectable only in pooled samples from the same age group. C_{28} VLC-PUFAs were undetectable even in pooled samples, suggesting that their levels were quite low. The C_{24}-C_{26} VLC-PUFAs in RPE/choroid were around one-third of that in retina, whereas C_{30}-C_{34} VLC-PUFAs were around one-tenth. Although there are no statistics provided in this portion of the study because samples had to be pooled, the trends of change of VLC-PUFAs in RPE/choroid with aging and AMD were similar to retina, peaking in middle age donors and severely decreased in AMD donors.

DISCUSSION

In this study, LC-FAs and VLC-PUFAs were systematically analyzed with regard to age and AMD status in human donor eyes with special emphasis on VLC-PUFAs, because low levels have recently been associated with *ELOVL4*-related retinal eye disease (42–44). No age-dependent change in the relative concentrations of the 26 LC-FAs was observed in total

retinal lipids (Table 2). Our results are consistent with previous studies (40, 45, 46) in which it was reported that concentrations of 16:0, 18:0, 18:1, 18:2, 18:3, 20:4, 22:4, 22:5, and 22:6 also are not altered with age in total phospholipids, which typically account for 74% of total retinal lipids. The levels of 16:0, 18:0, 20:4, and 22:6 in FFAs have been reported to have an increasing trend with age (47), but FFAs account for <10% of total lipid in retina. AA has been reported to increase in an age-dependent manner in human neural retina (48), but their study's age range (59–95 years) was markedly different from our study's age range.

Oxidative damage is postulated to be involved in AMD (49). The multiplicity of double bonds in DHA renders it extremely sensitive to free radical damage during oxidative stress (50). Crabb et al. demonstrated that carboxyethyl pyrrole (CEP) protein adducts, the oxidative protein modifications generated uniquely from the docosahexaenoate-containing lipids such as DHA and adrenic acid (51), are more abundant in ocular tissues from AMD retina than from normal retina (52). CEP biomarkers have been shown to enhance the AMD predictive accuracy of genomic AMD biomarkers (53, 54). The increase of CEP protein adducts in AMD retinas indicates that increased oxidation of DHA and adrenic acid that likely occurs in AMD eyes may lead to a reduction in DHA and adrenic acid, which is consistent with our study results. Dunaief et al. (55, 56) reported that retinas and RPE/choroid from AMD donor eyes exhibit marked accumulation of iron stores compared with age-matched normal donor tissue, which may lead to increased Haber-Weiss reactions

TABLE 4. VLC-PUFA composition from whole retinas collected from young, middle, and old age and age-matched AMD human donors

Peak no.[a]	RT (min)[b]	FAs[c]	Peak Area Value Normalized with IS and Sample Weight[d]			
			Young Age Group	Middle Age Group	Old Age Group	Age-Matched AMD Group
1	23.27	24:5n-6	185.24 ± 49.86	193.23 ± 41.19	147.60 ± 27.43	90.45 ± 18.65
2	23.43	24:6n-3	677.13 ± 237.78	668.48 ± 93.48	463.55 ± 55.82	151.65 ± 35.28[g]*
3	23.58	24:4n-6	1199.82 ± 315.71	1188.55 ± 142.75	1153.45 ± 210.28	684.20 ± 126.50
4	23.74	24:5n-3	1315.65 ± 537.16	1442.42 ± 246.56	1124.25 ± 199.82	468.76 ± 111.35
5	27.55	26:5-6	6.64 ± 2.46	10.74 ± 2.50	4.07 ± 0.99[f]*	3.49 ± 0.92
6	27.72	26:6n-3	25.77 ± 8.76	27.74 ± 4.07	23.73 ± 5.22	10.45 ± 1.78
7	28.00	26:4n-6	60.61 ± 14.54	74.85 ± 4.88	58.90 ± 17.90	23.34 ± 4.20[g]*
8	28.22	26:5n-3	57.07 ± 15.61	65.93 ± 6.25	46.70 ± 11.28	22.68 ± 4.36
9	33.61	28:6n-3	2.15 ± 0.61	2.09 ± 0.52	1.04 ± 0.45	0.13 ± 0.07
10	33.95	28:4n-6	2.54 ± 0.68	5.47 ± 0.72[e]*	2.63 ± 0.88[f]*	0.44 ± 0.24[g]*
11	34.42	28:5n-3	8.71 ± 2.16	10.25 ± 1.23	7.51 ± 3.25	0.93 ± 0.50[g]*
12	40.82	30:6n-3	2.62 ± 0.95	4.94 ± 0.93[e]*	2.07 ± 0.73[f]*	0.66 ± 0.26
13	41.42	30:4n-6	3.61 ± 1.08	6.84 ± 1.46	4.29 ± 1.79	0.90 ± 0.34[g]*
14	41.82	30:5n-3	5.57 ± 1.82	12.98 ± 2.16[e]*	4.93 ± 1.00[f]*	2.20 ± 0.70
15	48.84	32:5n-6	8.45 ± 2.76	14.30 ± 2.27	7.52 ± 2.40[f]*	1.51 ± 0.38[g]*
16	49.32	32:6n-3	31.36 ± 9.66	47.84 ± 5.48	25.11 ± 5.78[f]*	3.97 ± 0.97[g]*
17	50.00	32:4n-6	40.12 ± 11.35	80.71 ± 15.27[e]*	33.26 ± 8.27[f]*	9.20 ± 3.21
18	50.46	32:5n-3	20.20 ± 5.97	50.74 ± 9.02[e]*	21.53 ± 6.22[f]*	3.93 ± 1.35[g]*
19	58.49	34:6n-3	20.61 ± 8.43	25.94 ± 10.77	15.31 ± 3.80	1.71 ± 0.42
20	59.21	34:4n-6	25.37 ± 8.45	36.43 ± 5.76	16.50 ± 4.49[f]*	2.41 ± 0.77[g]*
21	59.72	34:5n-3	57.05 ± 28.08	105.06 ± 15.67	38.49 ± 16.01[f]*	7.35 ± 2.19
Ratio of n-6/n-3 VLC-PUFAs			0.83 ± 0.11	0.70 ± 0.11	0.83 ± 0.09	1.24 ± 0.10[g]*
Sum of all VLC-PUFAs			3757.77 ± 1205.26	4076.73 ± 458.17	3202.96 ± 535.34	1354.99 ± 268.34[g]*

[a] Peak no. was shown in chromatograms of Fig. 2.

[b] Retention time.

[c] Number of carbon atoms: number of double bonds, the position of first double bound.

[d] Mean ± SEM; young age group: n = 5, middle age group: n = 6, old age group: n = 5, age-matched AMD group: n = 8.

[e]* Significant differences ($P < 0.05$) between young and middle age group.

[f]* Significant differences ($P < 0.05$) between middle and old age group.

[g]* Significant differences ($P < 0.05$) between old and age-matched AMD age group.

whereby n-6 and n-3 PUFAs undergo oxidative degradation, resulting in generation of the corresponding active aldehydes such as CEP. Thus, accumulation of iron stores in AMD eyes may lead to oxidative degradation of PUFAs and subsequent CEP generation, which is consistent with our study results and Crabb et al. (51–53).

Besides oxidative damage, inflammation is also postulated to be involved in AMD (49). When inflammation happens, cytokines and chemokines stimulate phospholipase A2 and cyclooxygenases, which results in a breakdown of membrane glycerophospholipids with the release of DHA. Then, DHA is metabolized to resolvins and neuroprotectins, which can prevent inflammation by inhibiting transcription factor nuclear factor κB, prostaglandins, leukotrienes, and thromboxanes, preventing cytokine secretion and modulating leukocyte trafficking (57, 58). Therefore, in our study, reduction of DHA in AMD retinas may also be the result of anti-inflammatory processes.

The ratio of AA/DHA is increased in AMD ocular tissue compared with the age-matched normal group, suggesting an imbalance in pro- and anti-inflammatory processes in AMD retina. In accordance with our findings, a lower retinal n-6/n-3 PUFA ratio has a protective effect against pathological angiogenesis (59). All of these results suggest that oxidative stress and inflammation play an important role in the etiology of AMD (60), whereas a reduction in DHA and adrenic acid and an increase in the ratios of AA/DHA and n-6/n-3 may be biomarkers of AMD.

When we analyzed RPE/choroid LC-PUFAs, we noted some data with more variability relative to retina, perhaps due to the presence of contaminating blood lipids. LA in RPE/choroid was significantly higher in the old age group compared with the young and middle age groups, suggesting that LA might accumulate in RPE lipofuscin with age after being delivered to the RPE from the diet (61). Lower DHA in RPE/choroid than retina may be due to selective recycling of DHA into photoreceptor outer segment lipids (21, 62, 63). DHA and adrenic acid in RPE/choroid were higher in the normal old age group than in the AMD group, which was similar to findings in the retina. Such similarity between retina and RPE/choroid is likely due to RPE phagocytosis of approximately 10% of the photoreceptor outer segment material daily, because each photoreceptor renews its outer segment every 10 days (61, 64).

C_{24} and C_{26} VLC-PUFAs can be made from 22:4n-6 and 22:5n-3 (35, 36, 65) (supplementary Fig. I). Thus, the decrease of C_{24} and C_{26} VLC-PUFAs in AMD retinas compared with age-matched normal retinas is consistent with the decrease of 22:4n-6 and 22:5n-3. Many C_{28}-C_{34} VLC-PUFAs were significantly decreased in AMD retinas relative to age-matched normal retinas. This may be due to the lower level of precursors such as 22:4n-6 and 22:5n-3 in AMD retina or impaired enzymatic processing. C_{28}-C_{38} VLC-PUFAs can be converted from EFAs through the consecutive enzymatic activities of desaturases, elongases, and β-oxidation enzymes in mammals (31, 35, 36) (supplementary Fig. I), but elongation requires ELOVL4,
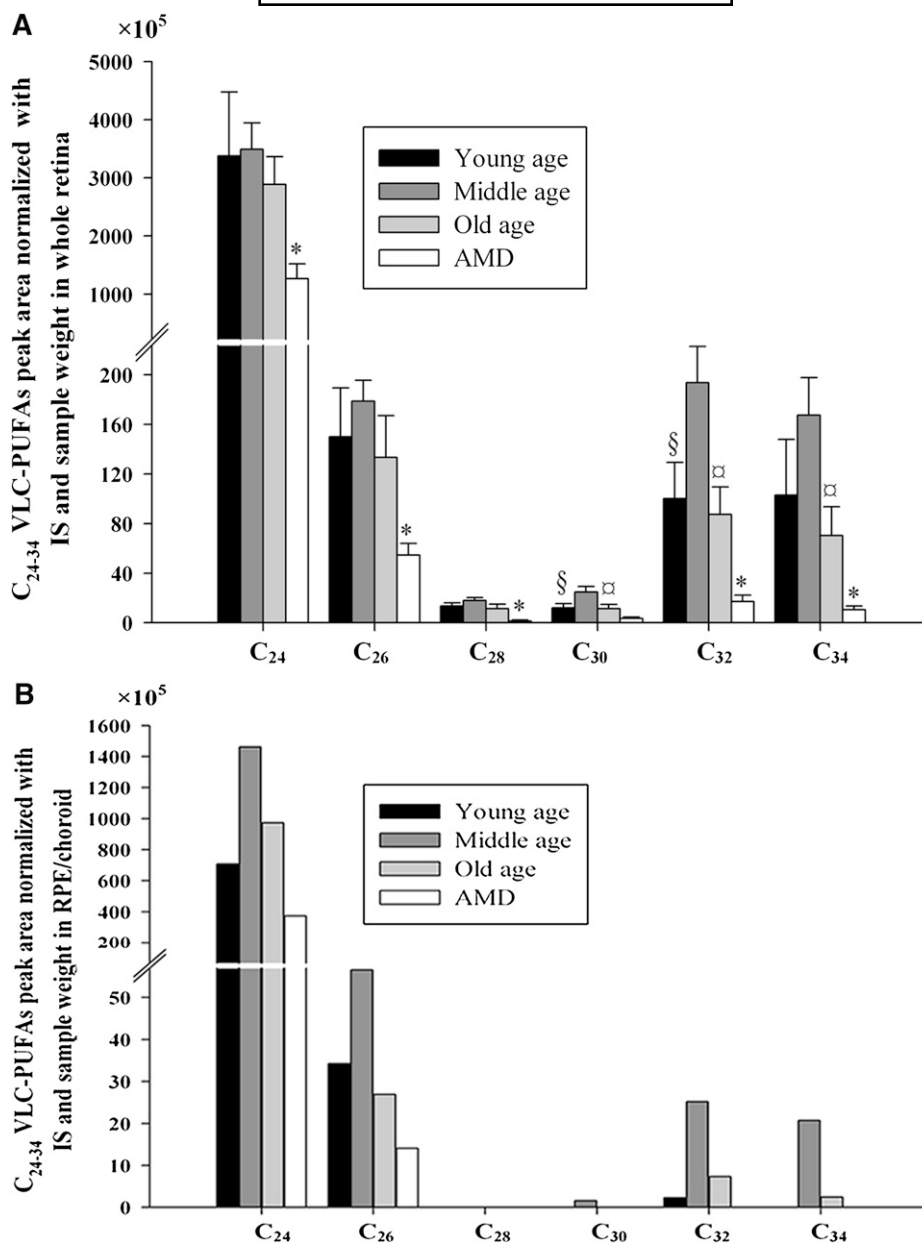
Fig. 4. Comparisons of C_{24}-C_{34} VLC-PUFAs in young age, middle age, and old age and age-matched AMD donors. A and B are the levels of C_{24}-C_{34} VLC-PUFAs in the whole retina and RPE/choroid, respectively, from young age, middle age, old age, and age-matched AMD donors. Statistical analysis was performed using SPSS statistical software. Statistical significance was determined by one-way ANOVA. §, Significant differences ($P < 0.05$) between young and middle age group; ¤, means significant differences ($P < 0.05$) between middle and old age group; *, significant differences ($P < 0.05$) between old and age-matched AMD group. In B, there are no statistics provided, because each group's samples had to be pooled. IS: internal standard.

which uniquely exists in retina, sperm, skin, testes, thymus, and brain (36) (supplementary Fig. I). Reduced levels of VLC-PUFAs are found in retinas of animal models of autosomal dominant Stargardt macular dystrophy, a macular dystrophy that results from truncating mutations of the *ELOVL4* gene (42), and the Met299Val variant in the *ELOVL4* gene has been reported to be possibly associated with AMD risk (66). Furthermore, just like DHA, more oxidization of VLC-PUFAs may also occur in AMD

retinas, which can reduce VLC-PUFAs in AMD retinas compared with normal retinas. The increased ratio of n-6/n-3 VLC-PUFAs in AMD retinas relative to normal retinas may also be due to differences in the relative levels of their n-6 and n-3 precursors.

In RPE/choroid, C_{24} and C_{26} VLC-PUFAs were detectable in all individual samples, whereas C_{30-34} VLC-PUFAs were at such low concentrations that they were detectable only in pooled samples, but they still exhibited

TABLE 5. VLC-PUFAs composition from pooled RPE/choroid collected from young, middle and old age and age-matched AMD human donors

Peak no.[a]	RT (min)[b]	FAs[c]	Peak Area Value Normalized with IS and Sample Weight[d]			
			Young Age Group	Middle Age Group	Old Age Group	Age-Matched AMD Group
1	23.27	24:5n-6	78.04	97.41	83.09	62.80
2	23.43	24:6n-3	147.30	376.30	259.11	66.48
3	23.58	24:4n-6	321.66	522.54	365.28	148.77
4	23.74	24:5n-3	161.86	465.52	266.57	96.15
5	27.55	26:5n-6	2.44	3.88	3.01	1.78
6	27.72	26:6n-3	6.63	12.73	6.23	1.68
7	28.00	26:4n-6	16.08	18.22	17.68	5.59
8	28.22	26:5n-3	9.11	21.72	14.83	5.02
9	33.61	28:6n-3	0.00	0.00	0.00	0.00
10	33.95	28:4n-6	0.00	0.00	0.00	0.00
11	34.42	28:5n-3	0.00	0.00	0.00	0.00
12	40.82	30:6n-3	0.00	0.37	0.00	0.00
13	41.42	30:4n-6	0.00	0.50	0.00	0.00
14	41.82	30:5n-3	0.00	0.70	0.00	0.00
15	48.84	32:5n-6	0.13	1.62	0.48	0.00
16	49.32	32:6n-3	0.78	8.12	2.23	0.00
17	50.00	32:4n-6	0.80	8.89	2.69	0.00
18	50.46	32:5n-3	0.54	6.52	1.94	0.00
19	58.49	34:6n-3	0.00	5.03	0.60	0.00
20	59.21	34:4n-6	0.00	4.58	0.46	0.00
21	59.72	34:5n-3	0.00	11.14	1.42	0.00
Ratio of n-6/n-3 VLC-PUFAs			1.28	0.72	0.85	1.29
Sum of all VLC-PUFAs			745.37	1565.79	1025.62	388.27

[a] Peak no. was shown in chromatograms of Fig. 2.
[b] Retention time.
[c] Number of carbon atoms: number of double bonds: position of double bonds, the position of first double bound.
[d] Average = peak area in pooled sample/n; young age group: n = 5, middle age group: n = 6, old age group: n = 5, age-matched AMD group: n = 8. No statistics are provided due to only one pooled sample in each group.

trends with age similar to retina. The RPE must phagocytize approximately 10% of the photoreceptor outer segment material daily insofar as each photoreceptor renews its outer segment every 10 days (61, 64), and each RPE cell underlies as many as 200 photoreceptors and may, therefore, ingest an equivalent of 20 entire outer segments per day (61, 64). This suggests that RPE/choroid may share the same C_{30-34} VLC-PUFAs with retina. This sharing between RPE/choroid and retina may explain our detection of C_{30-34} VLC-PUFAs in RPE/choroid at lower concentrations with distributions similar to overlying retina even though *ELOVL4* is absent in RPE/choroid (36). Interestingly, C_{28}-C_{34} VLC-PUFAs were below the limit of detection even in combined AMD RPE/choroid samples, correlating well with our retinal findings.

In summary, we have demonstrated that the human retina and RPE/choroid exhibit substantial alterations in PUFA levels with age and that these changes are magnified in AMD donor eyes. These alterations are especially prominent in lipids of the VLC-PUFA series in AMD eyes where these lipids are severely reduced in the retina and undetectable in the RPE/choroid, and n-6/n-3 ratios are increased. The underlying causes for these changes with age and disease remain to be elucidated, but they may originate from dietary alterations, decreased enzymatic synthesis, or accelerated breakdown of LC-PUFAs and VLC-PUFAs. Future studies should include donor eyes with a wider range of well-characterized AMD pathologies, because the current study utilized predominantly early and intermediate stage AMD eyes, and higher sensitivity GC-MS methods should permit study of regional variations of VLC-PUFAs in macular and peripheral regions of the retina. Our results support the potential value of interventions to increase retinal VLC-PUFAs and to decrease n-6/n-3 ratios in the prevention and treatment of AMD.

REFERENCES

1. Futterman, S., and J. S. Andrews. 1964. The fatty acid composition of human retinal vitamin A ester and the lipids of human retinal tissue. *Invest. Ophthalmol.* **3:** 441–444.
2. van Kuijk, F. J., and P. Buck. 1992. Fatty acid composition of the human macula and peripheral retina. *Invest. Ophthalmol. Vis. Sci.* **33:** 3493–3496.
3. Martinez, M., A. Ballabriga, and J. J. Gil-Gibernau. 1988. Lipids of the developing human retina: I. Total fatty acids, plasmalogens, and fatty acid composition of ethanolamine and choline phosphoglycerides. *J. Neurosci. Res.* **20:** 484–490.
4. Anderson, R. E. 1970. Lipids of ocular tissues. IV. A comparison of the phospholipids from the retina of six mammalian species. *Exp. Eye Res.* **10:** 339–344.
5. Benolken, R. M., R. E. Anderson, and T. G. Wheeler. 1973. Membrane fatty acids associated with the electrical response in visual excitation. *Science.* **182:** 1253–1254.
6. Wheeler, T. G., R. M. Benolken, and R. E. Anderson. 1975. Visual membranes: specificity of fatty acid precursors for the electrical response to illumination. *Science.* **188:** 1312–1314.

7. Greiner, R. S., T. Moriguchi, A. Hutton, B. M. Slotnick, and N. Salem, Jr. 1999. Rats with low levels of brain docosahexaenoic acid show impaired performance in olfactory-based and spatial learning tasks. *Lipids.* **34 (Suppl.):** S239–S243.

8. Rotstein, N. P., L. E. Politi, O. L. German, and R. Girotti. 2003. Protective effect of docosahexaenoic acid on oxidative stress-induced apoptosis of retina photoreceptors. *Invest. Ophthalmol. Vis. Sci.* **44:** 2252–2259.

9. Rotstein, N. P., L. E. Politi, and M. I. Aveldano. 1998. Docosahexaenoic acid promotes differentiation of developing photoreceptors in culture. *Invest. Ophthalmol. Vis. Sci.* **39:** 2750–2758.

10. Uauy, R., D. R. Hoffman, P. Peirano, D. G. Birch, and E. E. Birch. 2001. Essential fatty acids in visual and brain development. *Lipids.* **36:** 885–895.

11. Hibbeln, J. R., J. M. Davis, C. Steer, P. Emmett, I. Rogers, C. Williams, and J. Golding. 2007. Maternal seafood consumption in pregnancy and neurodevelopmental outcomes in childhood (ALSPAC study): an observational cohort study. *Lancet.* **369:** 578–585.

12. Innis, S. M., and R. W. Friesen. 2008. Essential n-3 fatty acids in pregnant women and early visual acuity maturation in term infants. *Am. J. Clin. Nutr.* **87:** 548–557.

13. Alessandri, J. M., P. Guesnet, S. Vancassel, P. Astorg, I. Denis, B. Langelier, S. Aid, C. Poumes-Ballihaut, G. Champeil-Potokar, and M. Lavialle. 2004. Polyunsaturated fatty acids in the central nervous system: evolution of concepts and nutritional implications throughout life. *Reprod. Nutr. Dev.* **44:** 509–538.

14. Weisinger, H. S., A. J. Vingrys, and A. J. Sinclair. 1996. The effect of docosahexaenoic acid on the electroretinogram of the guinea pig. *Lipids.* **31:** 65–70.

15. Uauy, R., P. Peirano, D. Hoffman, P. Mena, D. Birch, and E. Birch. 1996. Role of essential fatty acids in the function of the developing nervous system. *Lipids.* **31 (Suppl.):** S167–S176.

16. Connor, W. E., M. Neuringer, and S. Reisbick. 1992. Essential fatty acids: the importance of n-3 fatty acids in the retina and brain. *Nutr. Rev.* **50:** 21–29.

17. Neuringer, M., W. E. Connor, C. Van Petten, and L. Barstad. 1984. Dietary omega-3 fatty acid deficiency and visual loss in infant rhesus monkeys. *J. Clin. Invest.* **73:** 272–276.

18. Neuringer, M., W. E. Connor, D. S. Lin, L. Barstad, and S. Luck. 1986. Biochemical and functional effects of prenatal and postnatal omega 3 fatty acid deficiency on retina and brain in rhesus monkeys. *Proc. Natl. Acad. Sci. USA.* **83:** 4021–4025.

19. Neuringer, M., G. J. Anderson, and W. E. Connor. 1988. The essentiality of n-3 fatty acids for the development and function of the retina and brain. *Annu. Rev. Nutr.* **8:** 517–541.

20. Tinoco, J., M. A. Williams, I. Hincenbergs, and R. L. Lyman. 1971. Evidence for nonessentiality of linolenic acid in the diet of the rat. *J. Nutr.* **101:** 937–945.

21. Cho, E., S. Hung, W. C. Willett, D. Spiegelman, E. B. Rimm, J. M. Seddon, G. A. Colditz, and S. E. Hankinson. 2001. Prospective study of dietary fat and the risk of age-related macular degeneration. *Am. J. Clin. Nutr.* **73:** 209–218.

22. Sangiovanni, J. P., E. Agron, A. D. Meleth, G. F. Reed, R. D. Sperduto, T. E. Clemons, and E. Y. Chew. 2009. {omega}-3 Long-chain polyunsaturated fatty acid intake and 12-y incidence of neovascular age-related macular degeneration and central geographic atrophy: AREDS report 30, a prospective cohort study from the Age-Related Eye Disease Study. *Am. J. Clin. Nutr.* **90:** 1601–1607.

23. Parekh, N., R. P. Voland, S. M. Moeller, B. A. Blodi, C. Ritenbaugh, R. J. Chappell, R. B. Wallace, and J. A. Mares. 2009. Association between dietary fat and age-related macular degeneration in the Carotenoids in Age-Related Eye Disease Study (CAREDS): an ancillary study of the Women's Health Initiative. *Arch. Ophthalmol.* **127:** 1483–1493.

24. Tuo, J., R. J. Ross, A. A. Herzlich, D. Shen, X. Ding, M. Zhou, S. L. Coon, N. Hussein, N. Salem, Jr., and C. C. Chan. 2009. A high omega-3 fatty acid diet reduces retinal lesions in a murine model of macular degeneration. *Am. J. Pathol.* **175:** 799–807.

25. SanGiovanni, J. P., and E. Y. Chew. 2005. The role of omega-3 long-chain polyunsaturated fatty acids in health and disease of the retina. *Prog. Retin. Eye Res.* **24:** 87–138.

26. Seddon, J. M., S. George, and B. Rosner. 2006. Cigarette smoking, fish consumption, omega-3 fatty acid intake, and associations with age-related macular degeneration: the US Twin Study of Age-Related Macular Degeneration. *Arch. Ophthalmol.* **124:** 995–1001.

27. Hodge, W. G., D. Barnes, H. M. Schachter, Y. I. Pan, E. C. Lowcock, L. Zhang, M. Sampson, A. Morrison, K. Tran, M. Miguelez, et al. 2007. Evidence for the effect of omega-3 fatty acids on progression of age-related macular degeneration: a systematic review. *Retina.* **27:** 216–221.

28. Hubbard, A. F., E. W. Askew, N. Singh, M. Leppert, and P. S. Bernstein. 2006. Association of adipose and red blood cell lipids with severity of dominant Stargardt macular dystrophy (STGD3) secondary to an ELOVL4 mutation. *Arch. Ophthalmol.* **124:** 257–263.

29. Li, F., L. D. Marchette, R. S. Brush, M. H. Elliott, Y. Z. Le, K. A. Henry, A. G. Anderson, C. Zhao, X. Sun, K. Zhang, et al. 2009. DHA does not protect ELOVL4 transgenic mice from retinal degeneration. *Mol. Vis.* **15:** 1185–1193.

30. Hardy, S. J., A. Ferrante, A. Poulos, B. S. Robinson, D. W. Johnson, and A. W. Murray. 1994. Effect of exogenous fatty acids with greater than 22 carbon atoms (very long chain fatty acids) on superoxide production by human neutrophils. *J. Immunol.* **153:** 1754–1761.

31. Suh, M., and M. T. Clandinin. 2005. 20:5n-3 but not 22:6n-3 is a preferred substrate for synthesis of n-3 very-long-chain fatty acids (C24–C36) in retina. *Curr. Eye Res.* **30:** 959–968.

32. Poulos, A. 1995. Very long chain fatty acids in higher animals–a review. *Lipids.* **30:** 1–14.

33. Aveldano, M. I. 1987. A novel group of very long chain polyenoic fatty acids in dipolyunsaturated phosphatidylcholines from vertebrate retina. *J. Biol. Chem.* **262:** 1172–1179.

34. McMahon, A., and W. Kedzierski. Polyunsaturated very-long-chain C28–C36 fatty acids and retinal physiology. *Br J Ophthalmol.* Epub ahead of print. May 21, 2010.

35. Denic, V., and J. S. Weissman. 2007. A molecular caliper mechanism for determining very long-chain fatty acid length. *Cell.* **130:** 663–677.

36. Agbaga, M. P., R. S. Brush, M. N. Mandal, K. Henry, M. H. Elliott, and R. E. Anderson. 2008. Role of Stargardt-3 macular dystrophy protein (ELOVL4) in the biosynthesis of very long chain fatty acids. *Proc. Natl. Acad. Sci. USA.* **105:** 12843–12848.

37. Agbaga, M. P., M. N. Mandal, and R. E. Anderson. 2010. Retinal very long-chain PUFAs: new insights from studies on ELOVL4 protein. *J. Lipid Res.* **51:** 1624–1642.

38. Poulos, A., P. Sharp, H. Singh, D. Johnson, A. Fellenberg, and A. Pollard. 1986. Detection of a homologous series of C26–C38 polyenoic fatty acids in the brain of patients without peroxisomes (Zellweger's syndrome). *Biochem. J.* **235:** 607–610.

39. Hara, A., and N. S. Radin. 1978. Lipid extraction of tissues with a low-toxicity solvent. *Anal. Biochem.* **90:** 420–426.

40. Bazan, H. E., N. G. Bazan, L. Feeney-Burns, and E. R. Berman. 1990. Lipids in human lipofuscin-enriched subcellular fractions of two age populations. Comparison with rod outer segments and neural retina. *Invest. Ophthalmol. Vis. Sci.* **31:** 1433–1443.

41. Fellenberg, A. J., D. W. Johnson, A. Poulos, and P. Sharp. 1987. Simple mass spectrometric differentiation of the n-3, n-6 and n-9 series of methylene interrupted polyenoic acids. *Biomed. Environ. Mass Spectrom.* **14:** 127–129.

42. McMahon, A., S. N. Jackson, A. S. Woods, and W. Kedzierski. 2007. A Stargardt disease-3 mutation in the mouse Elovl4 gene causes retinal deficiency of C32–C36 acyl phosphatidylcholines. *FEBS Lett.* **581:** 5459–5463.

43. Zhang, K., M. Kniazeva, M. Han, W. Li, Z. Yu, Z. Yang, Y. Li, M. L. Metzker, R. Allikmets, D. J. Zack, et al. 2001. A 5-bp deletion in ELOVL4 is associated with two related forms of autosomal dominant macular dystrophy. *Nat. Genet.* **27:** 89–93.

44. Bernstein, P. S., J. Tammur, N. Singh, A. Hutchinson, M. Dixon, C. M. Pappas, N. A. Zabriskie, K. Zhang, K. Petrukhin, M. Leppert, et al. 2001. Diverse macular dystrophy phenotype caused by a novel complex mutation in the ELOVL4 gene. *Invest. Ophthalmol. Vis. Sci.* **42:** 3331–3336.

45. Anderson, R. E., R. M. Benolken, P. A. Kelleher, M. B. Maude, and R. D. Wiegand. 1978. Chemistry of photoreceptor membrane preparations from squid retinas. *Biochim. Biophys. Acta.* **510:** 316–326.

46. Russell, Y., P. Evans, and G. H. Dodd. 1989. Characterization of the total lipid and fatty acid composition of rat olfactory mucosa. *J. Lipid Res.* **30:** 877–884.

47. Nourooz-Zadeh, J., and P. Pereira. 1999. Age-related accumulation of free polyunsaturated fatty acids in human retina. *Ophthalmic Res.* **31:** 273–279.

48. Bretillon, L., G. Thuret, S. Gregoire, N. Acar, C. Joffre, A. M. Bron, P. Gain, and C. P. Creuzot-Garcher. 2008. Lipid and fatty acid profile of the retina, retinal pigment epithelium/choroid, and the

lacrimal gland, and associations with adipose tissue fatty acids in human subjects. *Exp. Eye Res.* **87:** 521–528.

49. Hollyfield, J. G., V. L. Bonilha, M. E. Rayborn, X. Yang, K. G. Shadrach, L. Lu, R. L. Ufret, R. G. Salomon, and V. L. Perez. 2008. Oxidative damage-induced inflammation initiates age-related macular degeneration. *Nat. Med.* **14:** 194–198.

50. Halliwell, B., and S. Chirico. 1993. Lipid peroxidation: its mechanism, measurement, and significance. *Am J Clin Nutr* **57 (5 Suppl.):** 715S–724S; discussion 724S–725S.

51. Crabb, J. W., M. Miyagi, X. Gu, K. Shadrach, K. A. West, H. Sakaguchi, M. Kamei, A. Hasan, L. Yan, M. E. Rayborn, et al. 2002. Drusen proteome analysis: an approach to the etiology of age-related macular degeneration. *Proc. Natl. Acad. Sci. USA.* **99:** 14682–14687.

52. Gu, X., S. G. Meer, M. Miyagi, M. E. Rayborn, J. G. Hollyfield, J. W. Crabb, and R. G. Salomon. 2003. Carboxyethylpyrrole protein adducts and autoantibodies, biomarkers for age-related macular degeneration. *J. Biol. Chem.* **278:** 42027–42035.

53. Gu, J., G. J. Pauer, X. Yue, U. Narendra, G. M. Sturgill, J. Bena, X. Gu, N. S. Peachey, R. G. Salomon, S. A. Hagstrom, et al. 2009. Assessing susceptibility to age-related macular degeneration with proteomic and genomic biomarkers. *Mol. Cell. Proteomics.* **8:** 1338–1349.

54. Ni, J., X. Yuan, J. Gu, X. Yue, X. Gu, R. H. Nagaraj, and J. W. Crabb. 2009. Plasma protein pentosidine and carboxymethyllysine, biomarkers for age-related macular degeneration. *Mol. Cell. Proteomics.* **8:** 1921–1933.

55. Dunaief, J. L., C. Richa, E. P. Franks, R. L. Schultze, T. S. Aleman, J. F. Schenck, E. A. Zimmerman, and D. G. Brooks. 2005. Macular degeneration in a patient with aceruloplasminemia, a disease associated with retinal iron overload. *Ophthalmology.* **112:** 1062–1065.

56. Hahn, P., A. H. Milam, and J. L. Dunaief. 2003. Maculas affected by age-related macular degeneration contain increased chelatable iron in the retinal pigment epithelium and Bruch's membrane. *Arch. Ophthalmol.* **121:** 1099–1105.

57. Farooqui, A. A., L. A. Horrocks, and T. Farooqui. 2007. Modulation of inflammation in brain: a matter of fat. *J. Neurochem.* **101:** 577–599.

58. Phillis, J. W., L. A. Horrocks, and A. A. Farooqui. 2006. Cyclooxygenases, lipoxygenases, and epoxygenases in CNS: their role and involvement in neurological disorders. *Brain Res. Rev.* **52:** 201–243.

59. Connor, K. M., J. P. SanGiovanni, C. Lofqvist, C. M. Aderman, J. Chen, A. Higuchi, S. Hong, E. A. Pravda, S. Majchrzak, D. Carper, et al. 2007. Increased dietary intake of omega-3-polyunsaturated fatty acids reduces pathological retinal angiogenesis. *Nat. Med.* **13:** 868–873.

60. Ding, X., M. Patel, and C. C. Chan. 2009. Molecular pathology of age-related macular degeneration. *Prog. Retin. Eye Res.* **28:** 1–18.

61. Elner, V. M. 2002. Retinal pigment epithelial acid lipase activity and lipoprotein receptors: effects of dietary omega-3 fatty acids. *Trans. Am. Ophthalmol. Soc.* **100:** 301–338.

62. Gordon, W. C., E. B. Rodriguez de Turco, and N. G. Bazan. 1992. Retinal pigment epithelial cells play a central role in the conservation of docosahexaenoic acid by photoreceptor cells after shedding and phagocytosis. *Curr. Eye Res.* **11:** 73–83.

63. Gordon, W. C., and N. G. Bazan. 1993. Visualization of [3H]docosahexaenoic acid trafficking through photoreceptors and retinal pigment epithelium by electron microscopic autoradiography. *Invest. Ophthalmol. Vis. Sci.* **34:** 2402–2411.

64. Bok, D., and R. W. Young. 1979. Phagocytic properties of the retinal pigment epithelium. *In* The Retinal Pigment Epithelium. K. M. Zinn and M. F. Marmor, editors. Cambridge, MA: Harvard University Press. 148–174.

65. Leonard A. E., P. S. Sprecher, Y. S. Huang. 2004. Elongation of long-chain fatty acids. *Prog. Lipid Res.* **43:** 36–54.

66. Conley, Y. P., A. Thalamuthu, J. Jakobsdottir, D. E. Weeks, T. Mah, R. E. Ferrell, and M. B. Gorin. 2005. Candidate gene analysis suggests a role for fatty acid biosynthesis and regulation of the complement system in the etiology of age-related maculopathy. *Hum. Mol. Genet.* **14:** 1991–2002.